The Report is Generated by DrillBit Plagiarism Detection Software

## *Submission Information*

| | |
|---|---|
| Author Name | Okka Adiyanto |
| Title | Hasil Cek_ Okka Adiyanto |
| Paper/Submission ID | 1973780 |
| Submitted by | perpustakaan.similarity@uad.ac.id |
| Submission Date | 2024-06-10 11:01:08 |
| Total Pages, Total Words | 10, 3997 |
| Document type | Research Paper |

## *Result Information*

Similarity **14 %**

1 10 20 30 40 50 60 70 80 90

Sources Type

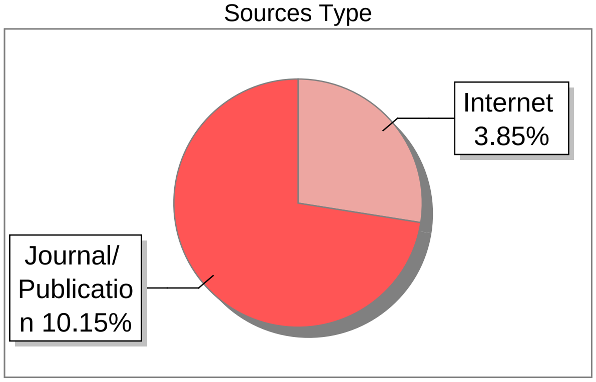


Report Content

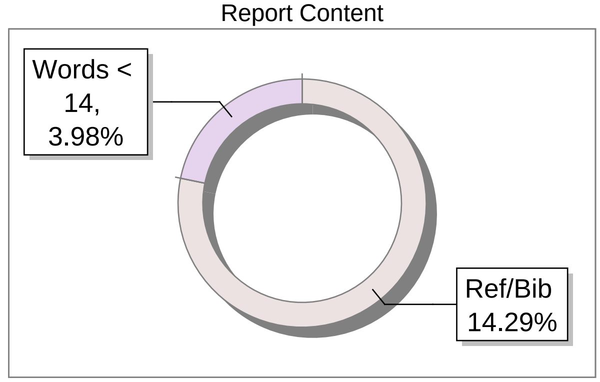


## *Exclude Information*

| | |
|---|---|
| Quotes | Excluded |
| References/Bibliography | Excluded |
| Source: Excluded < 14 Words | Not Excluded |
| Excluded Source | **0 %** |
| Excluded Phrases | Not Excluded |

## *Database Selection*

| | |
|---|---|
| Language | English |
| Student Papers | Yes |
| Journals & publishers | Yes |
| Internet or Web | Yes |
| Institution Repository | Yes |

A Unique QR Code use to View/Download/Share Pdf File

DrillBit

**DrillBit Similarity Report**

| 14 | 24 | B | A-Satisfactory (0-10%)<br>B-Upgrade (11-40%)<br>C-Poor (41-60%)<br>D-Unacceptable (61-100%) |
|---|---|---|---|
| SIMILARITY % | MATCHED SOURCES | GRADE | |

| LOCATION | MATCHED DOMAIN | % | SOURCE TYPE |
|---|---|---|---|
| 1 | journal.ump.edu.my | 3 | Publication |
| 2 | A Frequency-Based Interpretation of Energy-Based Model Reduction of Linear Syste by Louca-2016 | 1 | Publication |
| 3 | Sintering of AlSi10Mg particles in direct metal laser sintering process A molec by Nandy-2019 | 1 | Publication |
| 4 | The Finite Element Method in Engineering  Finite Element Analysis Us | 1 | Publication |
| 5 | uad.ac.id | 1 | Internet Data |
| 6 | www.dx.doi.org | 1 | Publication |
| 7 | www.emerald.com | 1 | Internet Data |
| 8 | moam.info | 1 | Internet Data |
| 9 | www.ije.ir | 1 | Publication |
| 10 | Biomass conversion of tamarind waste to syngas through gasification process on d by Aktawan-2019 | 1 | Publication |
| 11 | Qualification of electron-beam welded joints between copper and stainless steel  by Lusch-2015 | 1 | Publication |
| 13 | Kinetic Study of 1,5-Hydrogen Transfer Reactions of Methyl Acrylate and Butyl Ac by Xinru-2012 | <1 | Publication |

| | | | |
|---|---|---|---|
| 14 | Numerical modeling of the dynamic lateral behavior of geosynthetics-reinforced p by Taha-2015 | <1 | Publication |
| 15 | techscience.com | <1 | Internet Data |
| 16 | appliedmechanics.asmedigitalcollection.asme.org | <1 | Internet Data |
| 17 | journal.unair.ac.id | <1 | Internet Data |
| 18 | Study on the pyrolysis characteristics of walnut processing by-products by Xu-2020 | <1 | Publication |
| 19 | documents.mx | <1 | Internet Data |
| 21 | dochero.tips | <1 | Internet Data |
| 23 | scientific.net | <1 | Internet Data |
| 24 | www.dx.doi.org | <1 | Publication |
| 25 | biomedcentral.com | <1 | Internet Data |
| 26 | The impact of low birth weight and maternal age on adulthood offending by Vaske-2015 | <1 | Publication |
| 27 | ACM Press the 5th ACM Workshop- Roma, Italy (2013.11.11-2013.11.15, by Parisio, Alessandra- 2013 | <1 | Publication |

JOURNAL OF MECHANICAL ENGINEERING AND SCIENCES (JMES)
ISSN: 2289-4659 e-ISSN: 2231-8380
VOL. 14, ISSUE 3, 7152 – 7161
DOI: https://doi.org/10.15282/jmes.14.3.2020.16.0561

ORIGINAL ARTICLE

# Analysis of the vertical moving table type broaching machine

Okka Adiyanto[1], In Soo Park[2], Angga Senoaji H[3] and Won Sik Choi[2]

[1] Department of Industrial Engineering, Universitas Ahmad Dahlan, 55191, Bantul, Yogyakarta, Indonesia
[2] Department of Bio Industrial Machinery Engineering, Pusan National University,1268-50, Samnangjin-ro, Samnangjin-eup, Miryang-si, Gyeongsangnam-do, South Korea
[3] Badan Urusan Logistik Indonesia, 12950, Jakarta, Indonesia

**ABSTRACT** – Broaching is a type of machining that uses a toothed tool similar to a saw. There are several types of broaching machines includes linear broaching machines and hydraulic machines. Early linear broaching machines were driven mechanically by screws. However, hydraulic machines are faster, smoother in operation, and allow for high-speed steel broaches to be used. The purpose of this study is to an analysis of the vertical moving table type in the broaching machine. In this study, finite element analysis was carried out to examine the structural characteristics of broaching machine design. A model was created in CATIA software and analyzed with ANSYS to find the structural characteristics. The friction characteristic of PBT-40 material was also investigated. This material is recommended for guide rail surface lamination to reduce the friction coefficient and ram body wear. The simulation results provide information for the next step of development before physical prototype will be made. The maximum deformation of the workpiece table was 0.0517 mm on the positive Z-axis, and the maximum deformation on the pulling head device was 0.0598 mm on the negative Z-axis. The friction coefficients were between 0.013 and 0.047 in the sliding speed range of 0.06 to 0.34 m/s. The PBT-40 material has a wear coefficient of 1.604x10$^{-13}$ m$^3$/Nm according to the test. From the ANSYS friction simulation, it can be concluded that the PBT-40 material would not easily wear out during operation of the machine. It can be seen that small frictional stress occurred on the surface ranging from 8.273x10$^{-5}$ to 8.381x10$^{-5}$ MPa.

**ARTICLE HISTORY**
Revised: 07th Sep 2020
Accepted: 23rd Apr 2020

**KEYWORDS**
*Broach;*
*ANSYS;*
*CAD;*
*finite element analysis;*
*friction*

## INTRODUCTION

Broaching is a type of machining that uses a toothed tool similar to a saw, except the height of the teeth increases over the length of the tool. The broaching process can generate irregular internal and external part features Major Application of the broaching process is slotting, spline cutting, and production of internal helical gears [1]. Broaching is an ideal machining operation for a variety of applications due to its ability to produce complex features. The geometry of the broaching machined is derived directly by the inversion of tool geometry [2]. Parts of broaching machined have one linear cut along the surface of the workpiece so the broaching has simple dynamic properties, broaching machine is simple in construction because don't have a rotary motion [3,4]. Contact stress is very important in the evaluation in the some materials [5]

This process is commonly applied in precision machining on the surface of a workpiece. Its uses include circular or non-circular holes, splines, and keyways, and produces high surface quality with relatively short processing time. There are several types of broach machines, such as horizontal, vertical, and push or pull types. In the push or pulling type, it could be relative between the tool and the workpiece. In applications, it is possible to push or pull the workpiece with the tool. The scope of this study is the development of a Vertical Broach Machine (VBM), in which tools are clamped at the bottom and workpieces are pushed up by a hydraulic cylinder ram. The workpieces are positioned in the moving table (the ram body), which is attached to a hydraulic ram cylinder. The models of VBM are low as well as medium-cost machines, ideally used for mass production [6].

Abroach tends to be very expensive compared to other cutting tools, and it is not uncommon for a single broach to cost several thousand dollars to manufacture. This cost is a function of the design parameters, such as the number of rows of cutters. Proper broaching tool designs have 15 to 25 times faster cutting rates, but the broach life is decreased with higher speed [7]. Depth of cut, feed rate, and cutter geometry become parameters from the effect of the cutting process [8]. Cutting forces can be prediction during the machining process [9]. The broaching tool consists of multiple teeth separated by the thickness of one chip which causes to the removal of material [10].

Current modeling techniques and simulation tools provide engineers with a variety of options when it comes to the modeling of new or existing systems. These tools and techniques are powerful and extensively used in everyday engineering, but further improvements in modeling decisions and model complexity issues would make them more efficient. Specifically, the main disadvantage is that modeling techniques and simulation tools require sophisticated users who are often not domain experts and thus lack the ability to effectively utilize the available tools to uncover the important

*CORRESPONDING AUTHOR | Okka Adiyanto | okka.adiyanto@ie.uad.ac.id

design trade-offs [11]. A connecting part in a machine cannot be separated from friction. Surface contact between parts can become a crucial problem. The contact problem is nonlinear since the contact region is not known beforehand, and the boundary conditions may change during the analysis. Very few contact problems can be solved analytically, so they are generally solved with numerical techniques. The technique most used for structural nonlinearities is the finite element method (FEM) [12]. Finite element analyses (FEA) can reduce the cost of broach machine production [13].

FEA can investigate the critical buckling load like circular, square, elliptical (horizontal and vertical) and diamond [14]. FEM can analyze stress condition with different working condition, which improves the design efficiency and reduce the calculation error, FEM use of the constrained minimization methods [12], [15]. Computer-Aided Design (CAD) models and computer simulation software help designers to analyze and optimize a design, which reduces the cost and time needed for making a physical prototype [16]. ANSYS is a general-purpose finite element software that includes preprocessing to create the geometry and generate a mesh, as well as a solver and post-processing modules in a unified Graphical User Interface (GUI) environment. ANSYS commonly refers to ANSYS Mechanical or ANSYS Multiphysics Systems, where several parts can interact together and are subject to mechanical contact [17].

In this paper, static structural analysis was done using ANSYS for a vertical moving table-type broach machine. This paper analyzes several parts of the broaching machine, including stress and friction. Based on the results, the design of the broaching machine was optimized for the next step of development.

## BACKGROUND

Prior to making a physical prototype, we developed a virtual prototype. To develop this prototype, several analyses must be performed. The broach machine design is a pulling-type design. The machine works by pushing up the workpiece alongside the broach tools. The workpieces are put in the hydraulic ram attached to the ram body, and the tools are clamped to the pulling head. A schematic of the design can be seen in Figure 1.

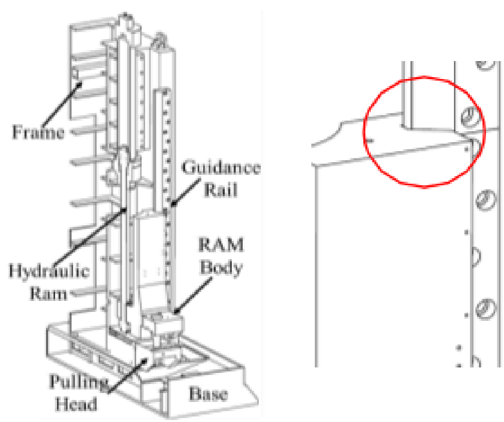


(a) (b)

**Figure 1.** (a) Cutaway of broach machine and (b) Ram body and guide rail

Figure 1(a) shows a cutaway of the broaching machine, and Figure 1**Error! Reference source not found.**(b) shows the broach ram body. This part can move up and down and is driven by a hydraulic ram. The ram body contacts the frame and is guided by a rail for to moving up and down. The contact surface between the ram body and the rail is separated with a PBT-40 material coating. The contact characteristics were investigated in prior research. The steps of development can be seen in Figure 2 First, a CAD model was designed. This model was used in the Multi Body System (MBS) analyses, FEA, and Command and Control (C&C) as an observation object.

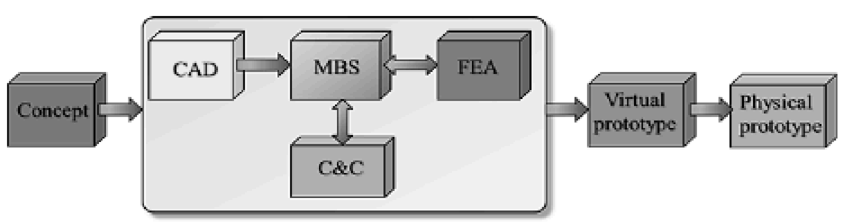


**Figure 2.** Schematic of development steps

The results were brought to a virtual prototype which is the final step before a physical prototype is made. The static structural analyses were divided into four parts. The first part is for the broach machine base at the contact area with the frame when a load is applied. The second is the friction characteristics between the moving table and the guide rail. The third is the characteristics of the moving table, which supports the workpieces when a load applied. This part is crucial since deformation can potentially occur. The last part is the pulling head section, which clamps the tools to fix them to the bottom.

## METHODOLOGY

The model was built from a technical design concept made with AUTOCAD software. The design was drawn in two dimensions and transferred into a three-dimensional model using CATIA software. The machine has a total height of 4593 mm, a base length of 2300 mm, and a base width of 1950mm. The hydraulic system and control box are installed separately, which can be seen in Figure 3.

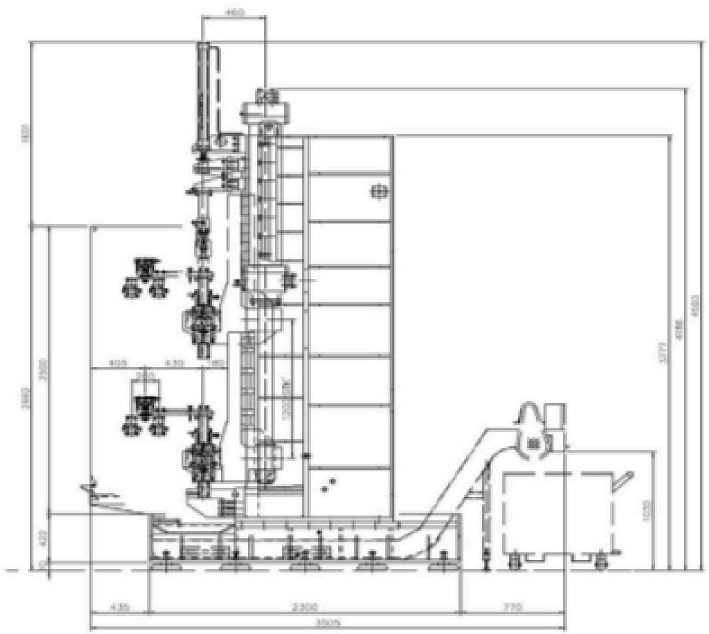

**Figure 3.** Two-dimensional broach machine drawing

After the three-dimensional model was built, it was used in ANSYS software for a static structural simulation test. To do the test, several boundary conditions were adapted from technical specifications for the design and applied to the model, which can be seen in Table 1.

**Table 1.** Boundary conditions

| Material | Steel |
|---|---|
| Density | 7850 kg/m$^3$ |
| Young's modulus | 2.1 x 10$^{11}$ Pa |
| Poisson ratio | 0.3 |
| Bulk modulus | 1.75 x 10$^{11}$ Pa |
| Shear modulus | 8.077 x 10$^{11}$ Pa |
| Tensile yield strength | 2.07 x 10$^8$ Pa |
| Compressive yield strength | 2.07 x 10$^8$ Pa |
| Tensile ultimate strength | 4.6 x 10$^8$ Pa |
| PBT-40 friction coefficient | 0.0247 |
| Ram body displacement | 700 mm |
| Hydraulic pressure | 5 MPa |
| Applied force | 10$^5$ N |

Model simplification was done to reduce the memory used for calculation before the test began. Half of the broach machine was analyzed symmetrically, as can be seen in Figure 1(a). The broach machine geometry and feature parameters were imported into the Design Modeler (DM) module of ANSYS workbench. The model was meshed by the DM module, and the boundary conditions were input. The results were the stress, total deformation, directional deformation, and results related to the broach machine structure. These results were used in the next steps of broach machine development, such as optimizing the design and building a physical prototype.

## RESULTS AND DISCUSSION

### Static Structural Results

The boundary conditions of the structural analyses that were applied to the model are shown in **Error! Reference source not found.**. Point A is fixed support. The frame and base have bonded-type conditions. At point B, an active force that is caused by the downward cutting force occurs in the ram body. $10^5$ N of force in the positive Z-axis direction was applied at this point. Points C and D are the hydraulic ram actuator connection and pulling head. These achieved $10^5$ N of load in the negative Z-axis direction. A hydraulic cylinder was attached at point E. It causes the frame to achieve a reaction force that is the same as point C but in the opposite direction. Point F is the cut section area, where free displacement is applied.

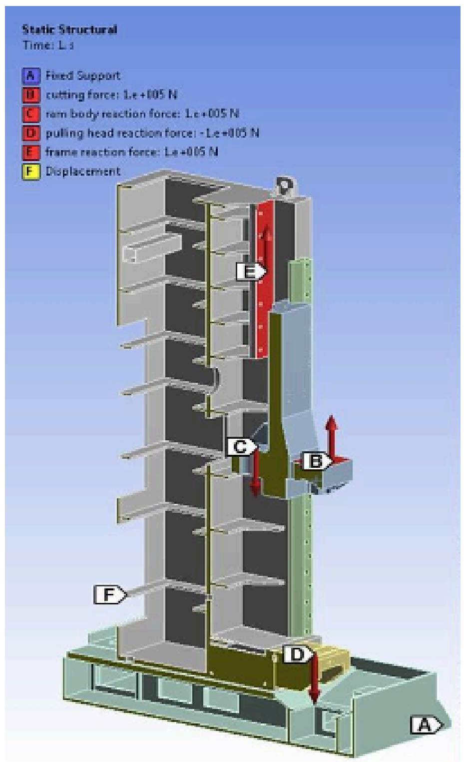


**Figure 4.** Model boundary conditions

The total body deformation on the Z-axis was analyzed using ANSYS Workbench. Deformations in several parts of the model were shown. The maximum deformation was 0.0517 mm, which occurred on the RAM-body work-piece table at point B. The minimum deformation of -0.0598 mm occurred at point D in the pulling head. The minus sign shows that the pulling head deformation has the opposite direction of the ram body deformation in the negative Z-axis coordinate. The pulling head has larger deformation than the ram body, and this part receives high compression when holding the workpiece. The ram body is the moving part and is driven with a hydraulic cylinder ram. The connection between them is shown by a circle in Figure 5(a). A deformation of -0.0027 mm occurred in this area, which was caused by the hydraulic ram pressure.

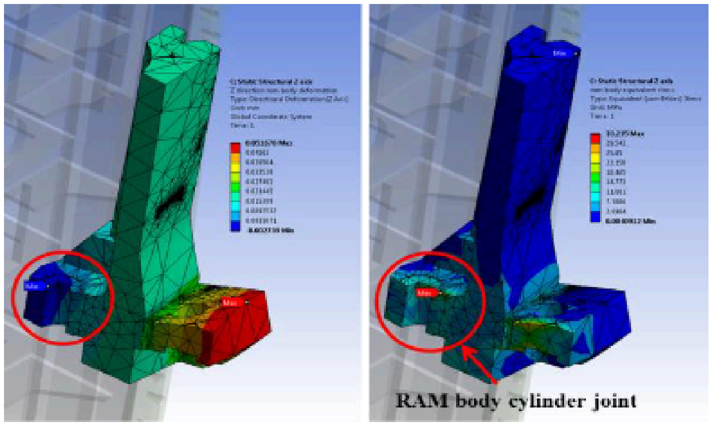


(a) (b)

**Figure 5.** (a) Deformation in the ram body and (b) von-Mises stress in the ram body

A von-Mises stress analysis for the ram body was performed, as shown in Figure 5(b). The results were 33.235 MPa for the maximum stress and 0.004 MPa for the minimum stress. The connection between the ram body and hydraulic ram has crucial conditions and is an important point in the design.

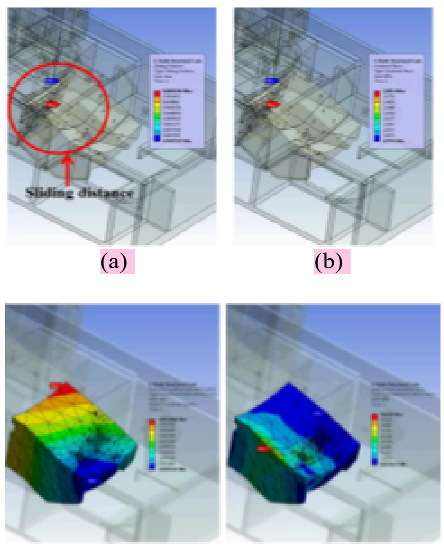


(a) (b)

(c) (d)

**Figure 6.** (a) Pulling head sliding distance, (b) pulling head frictional stress, (c) pulling head deformation and (d) pulling head von-Mises stress

The pulling head holds the workpiece during a broaching operation. It was attached to the mainframe with bolts, so it has high potential for sliding. This condition is shown in Figure 6(a), where sliding appears and is followed by frictional stress. During the broaching process, the pulling head slides 0.0058 mm and achieves frictional stress of 2.891 MPa, as shown in Figure 6(b). The pulling head deformation and von-Mises stress are shown in Figure 6(c) and Figure 6(d), respectively. The pulling head tends to bend inside of the symmetry area Y-positive axis), which is caused by the workpiece pressure. Hence, the symmetry corner achieved the maximum deformation of 0.0598 mm on the negative Z-axis with a von-Mises stress of 50.659 MPa.

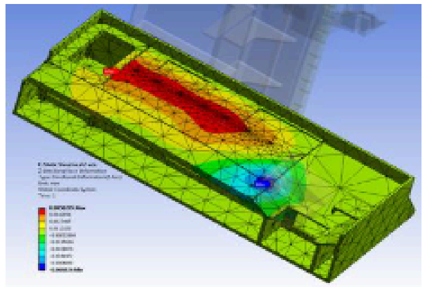

(a)

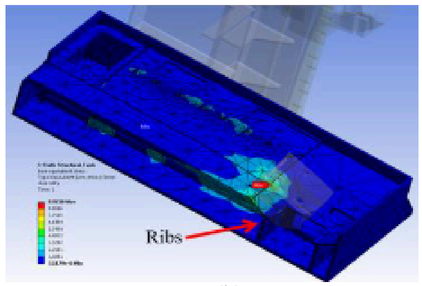


(b)

**Figure 7.** (a) Deformation on the base and (b) von-Mises stress on the base

The base structure deflected 0.0058 mm on the upper side and 0.0080 mm on the lower side. The front side of the base structure received higher pressure than the backside. This area is under the pulling head, so it needs more enforcement in the design. This was shown by the maximum von-Mises stress, which was 9.973 MPa. Ribs were added in this section to optimize the design.

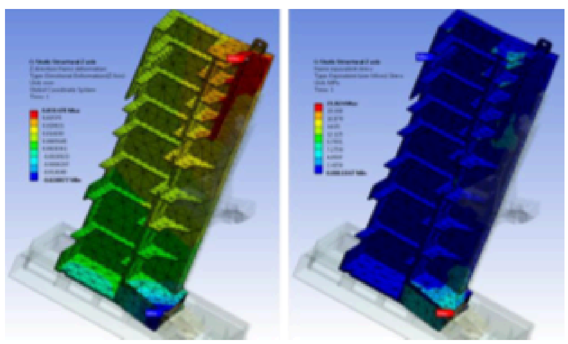

(a) (b)

**Figure 8.** (a) Deformation on the mainframe and (b) von-Misses stress on the mainframe

The broaching process was driven by a single hydraulic cylinder to push the ram body. This cylinder was tightly mounted with bolts on the upper mainframe, as seen in Figure 1(a). This point role plays the rigidity of the hydraulic cylinder. According to the ANSYS analyses, the hydraulic mounting has 0.0315 mm of deformation on the positive Z-axis. In the bottom of the mainframe, the deformation was 0.02 mm in the negative Z-axis direction. This condition is shown in Figure 8(a), and the von-Mises stress is shown in Figure 8(b). The maximum stress of 21.824 MPa occurred at the bottom of the mainframe in the negative Z-axis direction. On average, the stress of the upper section of the mainframe was small. The Summarize of deformation and von-Mises Stress can be seen Table 2.

**Table 2.** Deformation and stress each part

| | | |
|---|---|---|
| Deformation | RAM Body | Min 0.0027 mm<br>Max 0.0516 mm |
| | Pulling Head | Min -0.058 mm<br>Max -0.012 mm |
| | Base | Min 0.000026 mm<br>Max 0.0058 mm |
| | Main Frame | Min -0.02 mm<br>Max 0.0314 mm |
| von-Mises stress | RAM Body | Min 0.004 MPa<br>Max 33.235 MPa |
| | Pulling Head | Min 0.0256 MPa<br>Max 50.659 MPa |
| | Base | Min 3.817 MPa<br>Max 9.973 MPa |
| | Main Frame | Min 0.001184 MPa<br>Max 21.824 MPa |

## Friction Analyses

**Figure 9** shows the friction coefficients as a function of velocity for PBT-40 bearing tape in BW-BS-68 oil. The figure shows an overview of the frictional behaviour of the material. The range of the friction coefficient using BW-BS-68 lubricant is 0.0129 to 0.0474, and the coefficient decreases with increasing load. Based on Figure 9, the greater applied load, the greater friction will be generated. The variation of velocity will also be significant for the friction coefficient [18]. The greater the velocity the friction coefficient will be more constant. The variation of the velocity significantly affects the friction coefficient. At higher velocity, the friction coefficient has a constant tendency. This data was obtained using a sliding-type wear test machine. Sliding friction can be classified in two categories, the first is stationary and second is dynamic friction [19]. The stationary characteristic is typified by stribeck curve and dynamic characteristic by the friction coefficient. Focus in this study only dynamic characteristic.

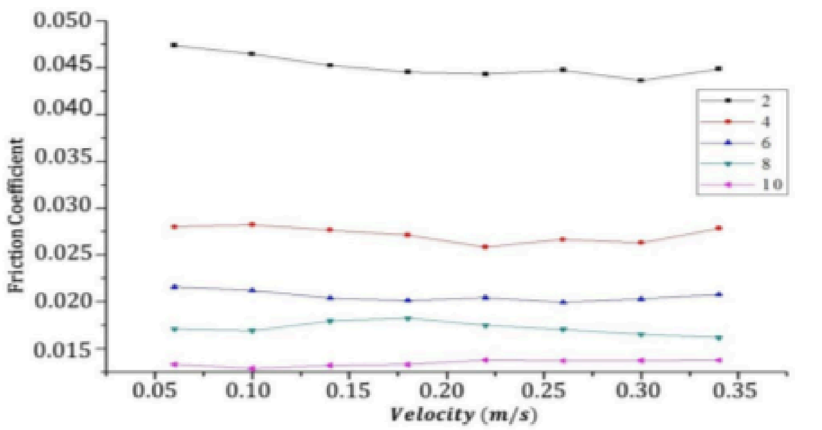


**Figure 9.** Friction coefficient as a function of velocity

The wear volume loss of the guide rail was calculated by measuring the weight of the specimen. The amount of wear is determined by measuring the appropriate linear dimensions of both specimens before and after the test. The wear volume of guide rail material is displayed in Figure 10.

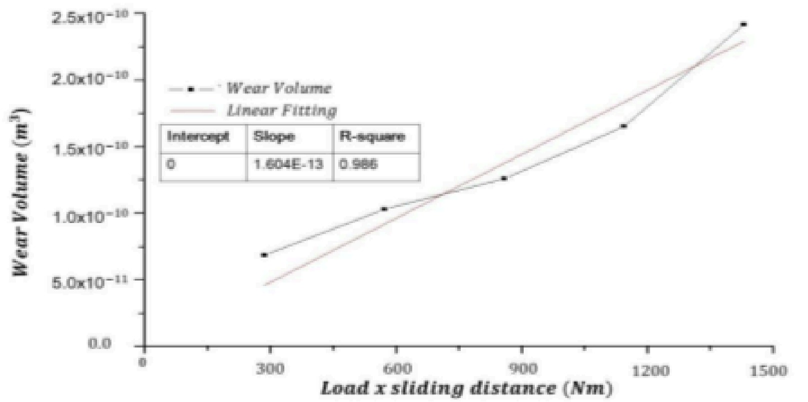


**Figure 10.** Wear volume of a guide rail

The wear rate coefficient was calculated using linear regression as $1.604 \times 10^{-13}$ $m^3$/Nm. An increase in the applied load increases the weight loss for the material in both zone, during sliding, the surface of the material is deformed under the applied force, and particles in the material are probably squeezed out, leading to a decrease in the contact area between the materials. This apparently leads to a decrease in the weight loss of the material [16]. The friction analyses were done by ANSYS according to the friction coefficient data in Figure 9. In the analyses, the friction coefficients were 0.01, 0.02, 0.03, and 0.04. The guide rail friction condition was analyzed in ANSYS. The contours of frictional stress and pressure are shown in Figure 11 and **Error! Reference source not found.**, and the maximum frictional stress and pressure are shown in **Table 3**.

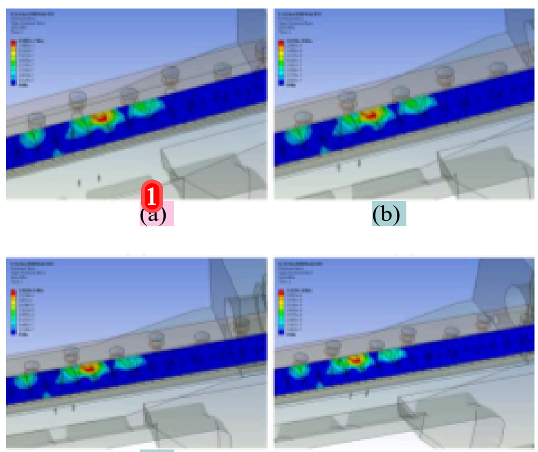
(a) (b) (c) (d)

**Figure 11.** Guide rail friction stress with several friction coefficients: (a) 0.01, (b) 0.02, (c) 0.03, and (d) 0.04

**Table 3.** Maximum frictional stress and pressure in guide rail

| Friction coefficient | Frictional stress (MPa) | Frictional pressure (MPa) |
|---|---|---|
| 0.01 | $8.389 \times 10^{-7}$ | $8.381 \times 10^{-5}$ |
| 0.02 | $1.677 \times 10^{-6}$ | $8.384 \times 10^{-5}$ |
| 0.03 | $2.452 \times 10^{-6}$ | $8.273 \times 10^{-5}$ |
| 0.04 | $3.316 \times 10^{-6}$ | $8.289 \times 10^{-5}$ |

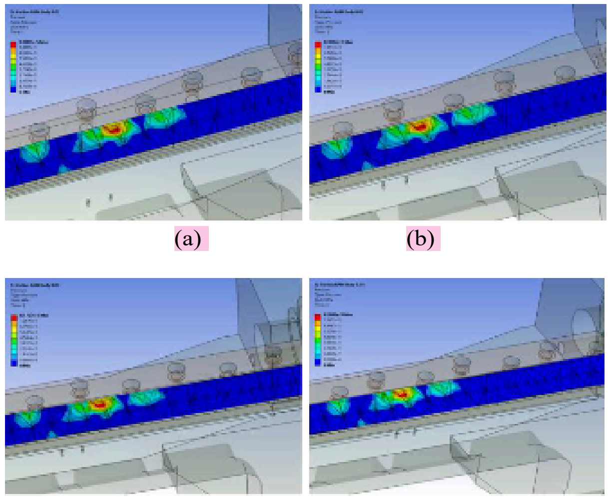

(a) (b) (c) (d)

**Figure 12.** Guide rail friction pressure with several friction coefficients: (a) 0.01, (b) 0.02, (c) 0.03, and (d) 0.04

The maximum frictional pressure in each condition has a constant tendency and ranged from $8.273\text{x}10^{-5}$ to $8.384\text{x}10^{-5}$ MPa. The frictional stress results have more variation. For each condition, the stress ranges from $8.389\text{x}10^{-7}$ to $3.316\text{x}10^{-6}$ MPa. Frictional stress increases gradually with the friction coefficient. However, changing the friction coefficient does not affect frictional pressure. According to these results, the broaching machine has acceptable structural design. Also, PBT-40 tape is recommended for the guide rail lamination layer.

## CONCLUSION

The important parts to be considered in the design are the ram body and pulling head device. The maximum deformation of the workpiece table was 0.0517 mm on the positive Z-axis, and the maximum deformation on the pulling head device was 0.0598 mm on the negative Z-axis. The frictional and pressure stress that occurred in the guide rail was small on average. According the friction test results, the ram body sliding speed affected the friction coefficient. The friction coefficients were between 0.013 and 0.047 in the sliding speed range of 0.06 to 0.34 m/s. The PBT-40 material has a wear coefficient of $1.604\text{x}10^{-13}$ $m^3$/Nm according to the test. From the ANSYS friction simulation, it can be concluded that the PBT-40 material would not easily wear out during operation of the machine. It can be seen that small frictional stress occurred on the surface ranging from $8.273\text{x}10^{-5}$ to $8.381\text{x}10^{-5}$ MPa. For this reason, PBT-40 material tape is recommended for the guide rail surface lamination. The friction characteristic of PBT-40 material was also investigated. This material is recommended for guide rail surface lamination to reduce the friction coefficient and ram body wear. The simulation results provide information for the next step of development before physical prototype will be made.

## REFERENCES


[1] L. Horace E, *Broaching : Tooling and Practice*, 1st ed. Industrial Press, 1961.

[2] A. Hosseini and H. . Kishaway, 'Prediction of Cutting Forces in Broaching Operation', *Journal of Advanced Manufacturing Systems*, vol. 12, no. 01, pp. 1–14, 2013.

[3] M. S. A. I. Kumar and M. Sagar, 'Design and Development of square Hole Broaching Machine', *International Journal of Engineering Research-Online*, vol. 6, no. 3, pp. 1–7, 2018.

[4] V. Schulze, N. Boev, and F. Zanger, 'Simulation of metal cutting process with variable cutting thickness during broaching', *Procedia CIRP*, vol. 1, no. 1, pp. 437–442, 2012.

[5] J. Eng, S. Karuppanan, and S. Patil, 'Frictional stress analysis of spur gear with misalignments', *Journal of mechanical engineering and Scinece*, vol. 12, no. 2, pp. 3566–3580, 2018.

[6] S. B. Herwade and A. M. Naniwadekar, 'Reliability Analysis of Vertical Broaching Machine by Fault Tree Analysis ( FTA ) Method', *International Journal for Innovative Research in Science & Technology*, vol. 3, no. 04, pp. 29–35, 2016.

[7] W. R. Terry and K. W. Cutright, 'Computer aided design of a broaching process', *Computers & Industrial Engineering*, vol. 11, no. 1–4, pp. 576–580, 1986.

[8] R. Kamath Cholpadi and A. Kuttan, 'Mechanistic Force Modeling for Broaching Process', *International Journal of Manufacturing Engineering*, vol. 2014, pp. 1–10, 2014.

[9] N. Sabkhi, C. Pelaingre, C. Barlier, A. Moufki, and M. Nouari, 'Characterization of the cutting forces generated during the gear hobbing process: Spur gear', *Procedia CIRP*, vol. 31, pp. 411–416, 2015.

[10] P. Vogtel, F. Klocke, D. Lung, and S. Terzi, 'Automatic broaching tool design by technological and geometrical optimization', *Procedia CIRP*, vol. 33, pp. 496–501, 2015.

[11] L. S. Louca, 'Modal analysis reduction of multi-body systems with generic damping', *Journal of Computational Science*, vol. 5, no. 3, pp. 415–426, May 2014.

[12] G. Hattori and A. L. Serpa, 'Contact stiffness estimation in ANSYS using simplified models and artificial neural networks', *Finite Elements in Analysis and Design*, vol. 97, no. January, pp. 43–53, 2015.

[13] S. Moaveni, *Finite Element Analysis Theory and Application with ANSYS*, vol. 2416514. 2007.

[14] S. B. Rayhan, 'A comprehensive study on the buckling behaviour of woven composite plates with major aerospace cutouts under uniaxial loading', *Journal of mechanical engineering and Scinece*, vol. 13, no. 2, pp. 4756–4776, 2019.

[15] S. Gu, 'Application of finite element method in mechanical design of automotive parts', *IOP Conference Series: Materials Science and Engineering*, vol. 231, no. 1, 2017.

[16] O. Adiyanto, P. S. Pratama, and W. Choi, 'Tribological characteristics of SCM 440 bearing steel under gas and oil lubricant in the cylinder block tractor engine', *Industrial Lubrication and Tribology*, vol. 70, no. 8, 2018.

[17] J. W. Sutherland, E. J. Salisbury, and F. W. Hoge, 'A model for the cutting force system in the gear broaching process', *International Journal of Machine Tools and Manufacture*, vol. 37, no. 10, pp. 1409–1421, Oct. 1997.

[18] N. Kaushik, S. Singhal, R. Rajesh, P. Gahlot, and B. N. Tripathi, 'Experimental investigations of friction stir welded AA6063 aluminum matrix composite', *Journal of Mechanical engineering and sciences*, vol. 12, no. 4, pp. 4127–4140, 2018.

[19] P. Sandi Pratama, D. Supeno, J. Y. Byun, and C. Wonsik, 'Tribology Characteristics of PBT-40 as RAM Body Lamination Material on Horizontal Surface Type Broaching Machine', in *Conference Material*, 2018, p. 4.